

AN EXPERIMENTAL AND NUMERICAL INVESTIGATION ON A DOVETAIL NOTCHED CONNECTION FOR CROSS-LAMINATED-TIMBER-CONCRETE COMPOSITE SLABS

Vanthet Ouch¹, Piseth Heng², Hugues Somja³, Thierry Soquet⁴

ABSTRACT: A specific dovetail notched connection has been proposed for CLT-concrete composite slabs. The particularity of this notched connection is its dovetail shape that provides a mechanical locking to limit the uplift without metallic screws. The experimental pushout results showed high stiffness and resistance. However, low ductility was obtained due to the failure by rolling shear of CLT. The performance and failure mechanism of the notched connector can be influenced by numerous variables. This paper presents a numerical study on the effect of different parameters related to the geometry and material properties, on the performance of the notched connection. First, an advanced 3-dimensionnal finite element model of the experimental test considering the nonlinear properties of the materials and the orthotropic behaviour of the CLT has been developed. The results of this model were validated against the experimental ones obtained from static pushout tests. A good agreement of the force-slip curves was obtained, and the model was able to reproduce the failure observed in the tests. Having validated the FE model, the parametric study was conducted to better understand the notched connector under the influence of variations in geometrical and material properties. Two different failure modes were obtained : the concrete shear at the notch and the rolling shear of the cross-layer of the CLT panel. The rolling shear failure of the CLT panel should be avoided in order to improve the post peak-performance of the notched connector. Reducing the notch length and increasing the heel length provoke the concrete shear failure of the notch, which improves the ductility of the connector if sufficient V-shape rebars are placed inside the notch. The stiffness of the connector can be influenced by changing the parameters such as the concrete resistance, the thickness of the concrete panel, the amount of V-shape rebars, the notch length and the heel length.

KEYWORDS: Dovetail notched connector, Pushout test, Parametric study, CLT-concrete composite slabs.

1 INTRODUCTION

Being responsible for around 39 percent of all carbon emissions around the world, the building and construction sectors are considered as the main contributor to the climate change [1]. The devastating consequences of climate changes urge the involved organizations to revolutionize building materials and construction methods in order to achieve 100 percent net zero emissions buildings by 2050. With such an objective, sustainable solutions for buildings have been widely studied. As an alternative to the traditional concrete or timber structures, Timber Concrete Composite (TCC) slabs might be an interesting solution that balance environmental impacts with structural and economical performances. A TCC slab is formed by laying a concrete panel on top of a timber panel and connecting them together using shear connection systems. This combination benefits the high performances of concrete in compression and of timber in tension. The structural

response of the composite system is ordinarily governed by the strength, stiffness, and ductility performance of the connection system.

Different types of shear connection systems have been developed in the past including steel fasteners, notches, and glue in order to enhance structural performance and cost-efficiency of TCC structures [2]. Among them, notched connection might be considered as the most effective system due to its high strength, stiffness as well as construction convenience. However, for this notched connection, steel fasteners are in general inserted in the timber and connected to the concrete notch to improve the shear strength and ductility of the connection as well as the uplift resistance between the concrete and timber. These steel fasteners are expensive and time-consuming in the construction process.

In response, a dovetail notched connection for CLT-concrete composite slabs has been proposed by T. Soquet and investigated by the authors [3]. The particular shape

¹ Vanthet Ouch, LGCGM/Structural Engineering Research Group, INSA de Rennes, France and Department of Civil Engineering, Institute of Technology of Cambodia, vanthet.ouch@insa-rennes.fr

² Piseth Heng, LGCGM/Structural Engineering Research Group, INSA de Rennes, France, piseth.heng@insa-rennes.fr

³ Hugues Somja, LGCGM/Structural Engineering Research Group, INSA de Rennes, France, hugues.somja@insa-rennes.fr

⁴ Thierry Soquet, Architecture Plurielle agency, Rennes, France, t.soquet@archi-plurielle.com

of the proposed notch configuration provides a geometrical constraint to limit the uplift without the need for metallic elements (see Figure 1). Experimental pushout tests have been conducted to determine the mechanical properties of the notched connection. It was found that the connection system showed high strength and stiffness with brittle failure due to the limited rolling shear resistance of the cross-layers of the CLT panel.

This paper presents a numerical study on this notched connection using Abaqus/Explicit [4] in order to determine the influence of selected parameters on the behaviour of the notched connection. First, a 3D FE model of the pushout test was developed and validated against the experimental results. Then, a parametric study on the variables defining the geometry and the materials was carried out.

2 SUMMARY OF THE EXPERIMENTAL WORK

2.1 MATERIAL CHARACTERISATION

The concrete was tested to determine the actual properties on the same day as pushout tests. Two series of three-cylinder specimens with a dimension of 11×22cm were tested for compressive strength f_{cm} and tensile strength f_{ct} . Table 1 presents the results obtained from concrete characterisation.

Table 1: The results obtained from the concrete test

Test	f_{ct} [MPa]	f_{cm} [MPa]
1B-1	3.20	34.51
1B-2	2.56	29.12
1B-3	3.39	39.51
Average (Var.)	3.05 (0.36)	34.38 (4.24)

CLT panels TOT'm X [5] were used. They are constituted of wooden planks with a thickness of 33 mm each, stacked in crossed layers at 90° and glued together over their entire surfaces (except the edge surfaces). Small-scale characterisation tests including longitudinal compression tests and rolling shear tests were conducted. The longitudinal compression tests were carried out in accordance with EN 408 [6] on 12 samples while the rolling shear tests using a configuration proposed in previous research [7] were carried out on 5 samples with three lamination layers (one cross layer sandwiched by two longitudinal layers). These samples had dimensions of 99 mm thick by 140 mm large by 269 mm long. Table 2 presents the value of longitudinal compression strength $f_{c,0}$, rolling shear strength f_v , and rolling shear modulus G_r obtained from characterisation test.

Table 2: The results obtained from the timber test

Test	$f_{c,0}$ [MPa]	G_r [MPa]	f_v [MPa]
Avg.	31.26	127	1.49
(Var.)	(5.33)	(25)	(0.17)

Steel rebars for the concrete panel and the notch connector have a nominal yield strength of 500 MPa.

2.2 RESULTS OF PUSHOUT TESTS

A series of three identical symmetrical pushout tests (1B-1, 1B-2 and 1B-3) were performed in order to determine the shear resistance, the stiffness, the deformation capacity and the failure mode of the dovetail notched connectors. The dimensions of the three specimens are presented in Figure 1. Specimen 1B-1 has a width of 500 mm, whereas specimens 1B-2 and 1B-3 have a width of 400 mm. The specimen was placed vertically on a support table, and the load was applied on the top surface of the CLT panel using a force jack with the capacity of 1500 kN (see Figure 2a). The test procedure described in Annex B of Eurocode 4 part 1-1 (2004) [8] was followed. The relative slip at the contact layer between concrete and timber panel was measured using Digital Image Correlation method with a precision of ± 0.1 mm. Two cameras were employed to record the relative displacements in the back face and the front face of the tested specimens.

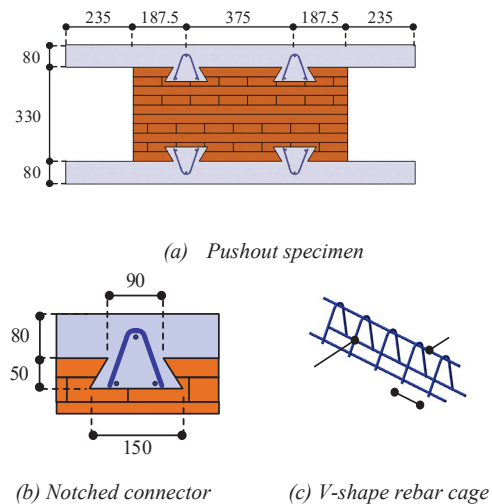


Figure 1: Configuration of pushout specimen (unit in mm)

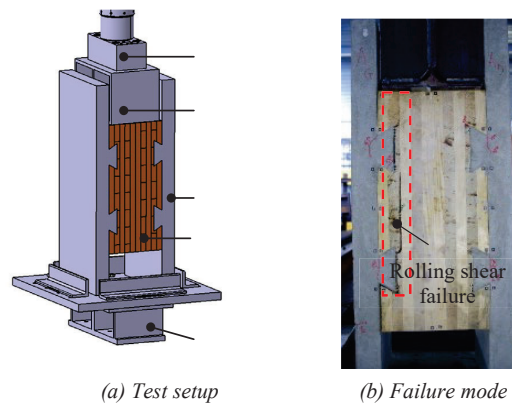


Figure 2: Description of pushout test setup and failure mode

Figure 3 and Table 3 present the force-slip curves and the results obtained from the pushout tests, respectively. The test results showed high shear resistance and stiffness for all the three tested specimens. However, a low ductility

was obtained, as the failure mode was governed by the shear failure of one cross-layer of the CLT panel (see Figure 2b). The maximum relative slip obtained from the experimental tests ranged between 0.8 mm and 1.6 mm. The maximum loads attained per connector per meter width (F_{max}) were 420 kN/m, 428 kN/m and 464 kN/m for test 1B-1, 1B-2 and 1B-3, respectively. The slip modulus to be used at serviceability limit state (SLS) K_s and ultimate limit state (ULS) K_u reported in Table 3 were computed following the method proposed by Ceccotti [9].

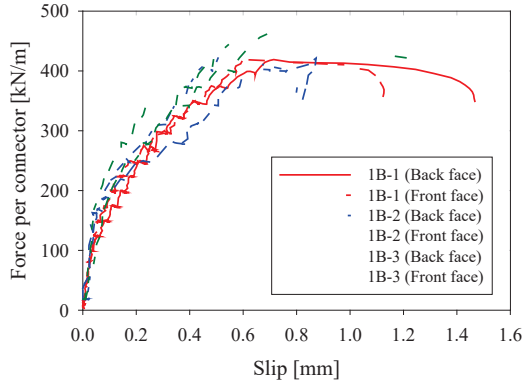


Figure 3: Load-slip curve of pushout tests

Table 3: The results for one connector per one meter linear

Test	F_{max} (kN/m)	$\delta_{F_{max}}$ (mm)	K_s (N/mm/m)	K_u (N/mm/m)
1B-1	420	0.79	1.81×10^6	1.41×10^6
1B-2	428	1.02	1.38×10^6	0.85×10^6
1B-3	464	0.90	1.29×10^6	1.10×10^6
Avg.	437		1.49×10^6	1.03×10^6

3 NUMERICAL STUDY

As mentioned above, the numerical study is divided into two steps. The first step consists of developing a 3D FE model of the experimental pushout test using ABAQUS/Explicit. The results of this model are validated against the experimental results. In the second step, the validated model serves to carry out a parametric study on the influence of various parameters on the behaviour of the notched connection.

3.1 MODEL ESTABLISHMENT

3.1.1 Geometry and boundary condition

To improve the computation speed, only one fourth of the test configuration was considered by taking advantages of the symmetric disposition and boundary conditions. All the components of the specimen as well as the steel loading block were modelled (see Figure 4a). The symmetric boundary conditions were applied at the highlighted surfaces in red and in blue colour (See Figure 4b), constraining the displacements in X-direction and Z-direction, respectively.

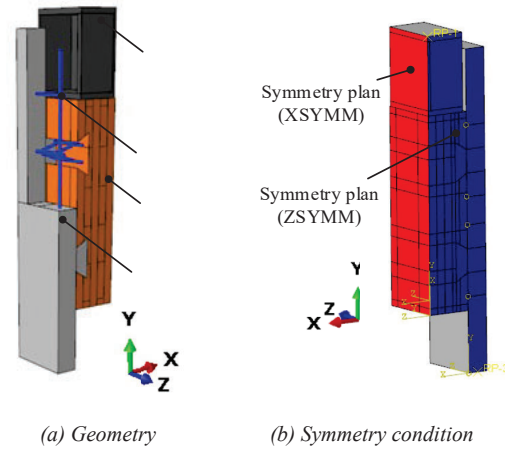


Figure 4: Geometry and symmetry condition of the FE model

The support was modelled by applying a rigid constraint to the bottom surface of the concrete panel that rigidly follows the movement of a reference point (see Figure 5a). All the degrees of freedom of this reference point were fixed.

The loading was simulated by applying an imposed displacement to another reference point that governs a rigid displacement of the top flange of the loading block HEA-300 (see Figure 5b).

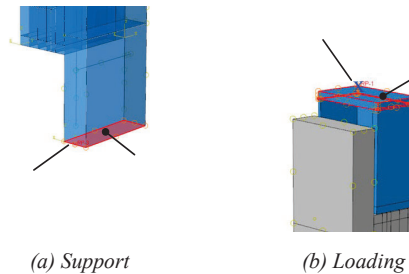


Figure 5: Support and Loading condition of the FE model

3.1.2 Material modelling

Concrete was considered as a non-linear isotropic material [10]. The concrete damaged plasticity (CDP) model available in Abaqus/Explicit was adopted [11] to reproduce properly the two main behaviours of concrete (compression crushing and tensile cracking). The actual concrete strength obtained from cylinder tests was used. Moreover, the parameters to define the flow potential and the yield surface including the dilatation angle Ψ , the eccentricity ϵ , the ratio of biaxial compressive strength to uniaxial compressive strength f_{b0}/f_{c0} , the shape factor for yield surface K_c , and the viscosity parameter μ were defined as in Table 4.

Table 4: Parameters of concrete damaged plasticity model

Ψ [°]	ϵ	f_{b0}/f_{c0}	K_c	μ
40	0.1	1.16	0.67	0

Timber was considered as an orthotropic material using the assumption that the stiffness and the strength in radial

and in tangential directions were identical. The mechanical stiffnesses were derived from the technical specification [5] except the rolling shear modulus G_r . The latter was taken from a specific shear test (see Table 5).

Table 5: Mechanical stiffnesses of the timber

E_1 (MPa)	$E_2=E_3$ (MPa)	$G_{12}=G_{13}$ (MPa)	G_{23} (MPa)	ν (-)
11000	370	690	127	0

Note: The subscription 1,2,3 refer to longitudinal, transversal, and radial directions, respectively.

The plasticity of the timber was defined using the orthotropic yield criteria proposed by Hill [12]. This criterion is an extension of Von-Mises yield criterion that consider the orthotropic behavior of the material. The stress potentials are related to the compressive strength parallel to grain $f_{c,0}$ and the shear strength of the timber f_v [13]. The timber strength was adopted from the characterization tests with $f_{c,0}=31$ MPa and $f_v=1.49$ MPa. Therefore, the six input parameters in ABAQUS were determined and are presented in Table 6.

Table 6: Stress potentials adopted in the FE model

R11	R22	R33	R12	R13	R23
1	0.0965	0.0965	0.22	0.22	0.084

Steel rebars were considered to be an isotropic material and to exhibit a bilinear elastic-plastic behaviour in the FE model. Properties based on experimental tests from literature [14] were used and are summarized in Table 7.

Table 7: Tensile properties of steel reinforcement

f_y (MPa)	f_u (MPa)	E (GPa)	ϵ_y [-]	ϵ_u [-]
500	635	200	0.00317	0.14559

3.1.3 Mesh definition and contact interaction

The concrete panel, the CLT panel and the HEA-300 loading block were meshed using hexahedral element with reduced integration and hourglass control (C3D8R) while the steel rebars were modelled using two-node beam element, B31. A finer mesh (5 mm) was generated in the neighbouring region of the connection system (see Figure 6). The rest had a size of 10 mm.

Surface-to-surface contact between concrete panel and CLT panel as well as between loading block (HEA 300) and CLT panel (see Figure 7) had to be considered. The contact properties were defined by hard contact and friction penalty formulations for the normal and tangential behaviours, respectively. In this study, the friction coefficient for the contacts between concrete and timber, and between steel and timber were 0.62 [15] and 0.50 [16], respectively. Apart from that, an embedded constraint was adopted for the interaction between the steel reinforcement and the concrete panel.

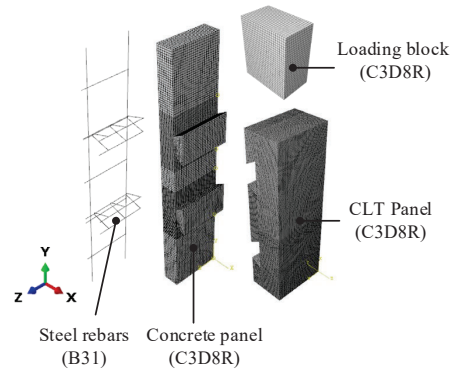


Figure 6: The mesh of components in the FE model

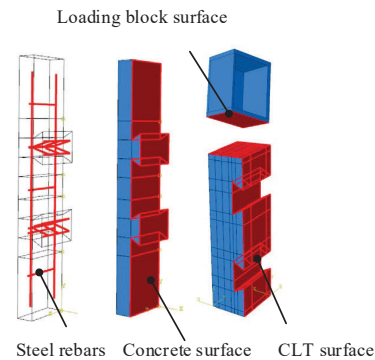


Figure 7: Contact surface of each component in the FE model

3.2 MODEL VALIDATION

The failure mode from the simulation was governed by the rolling shear failure of the CLT panel, reproducing the same failure mode as in experimental tests. Figure 8a,b illustrates the deformed shape and rolling shear stress at a maximum load obtained in FE model. Due to the configuration of the loading block that covers all the top surface of the CLT panel, a part of the load was transferred directly to the concrete notch in form of compressive force in the longitudinal layer and the rest was transmitted via rolling shear action of the cross-layers (see Figure 8c). Therefore, the real rolling shear resistance should be lower than the maximum force obtained in the test.

Figure 9a presents the comparison of force-slip curves obtained from the FE model and from the experimental tests. It can be seen that the FE model estimated a peak load at around 431 kN that is in good agreement with the experimental value, with approximately 2 percent difference. However, the behaviour of the notched connector in the FE model is stiffer, as smaller slip was obtained at the peak load compared to the experimental results. In fact, during the experimental tests, several cyclic loadings were applied, and rather frequent pauses were taken to observe the cracking in the concrete. This has generated additional slips due to additional creep strains. In order to be able to compare the results with the ones from the FE model, the slips caused by the cyclic loadings and the pauses were removed from the results. Figure 9b presents the new load-slip curves. A better

agreement of the curves was obtained. The comparison between the results obtained from FE model and the ones from experimental tests are summarized in Table 8. The differences of maximum force F_{max} and corresponding slip $\delta_{F_{max}}$ were respectively 2 percent and 3 percent while higher discrepancies of slip modulus were noticed with 22 percent and 8 percent for the values at SLS and at ULS, respectively. The precision of the Digital Image Correlation technique adopted in the pushout tests was 0.1 mm. Hence, it is difficult to obtain accurate experimental values of the slip modulus, as the connection is very stiff.

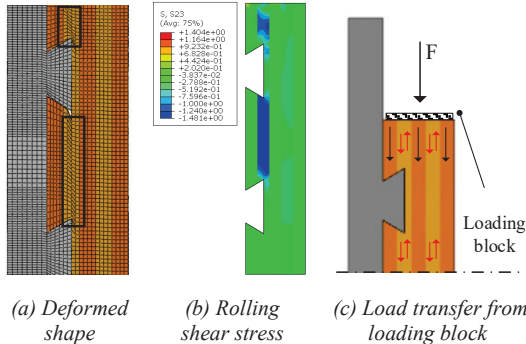
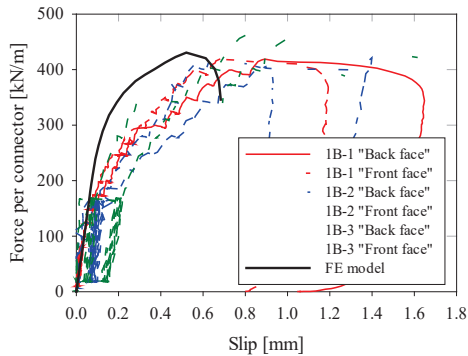
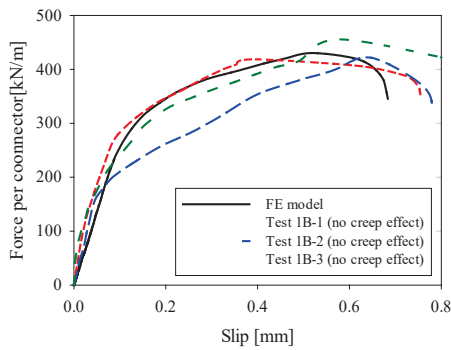


Figure 8: Deformed shape of the cross-layer, rolling shear stress, and load transfer mechanism from loading block in the FE model



(a) Original experimental load-slip curves



(b) Modified Load-slip curves

Figure 9: Comparison of load-slip curves

Table 8: Results of the FE model and experimental tests

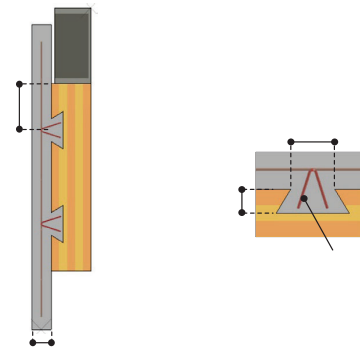
Test	F_{max} [kN/m]	$\delta_{F_{max}}$ [mm]	K_s [N/mm/m]	K_u [N/mm/m]
1B-1	420	0.39	3.92×10^6	3.22×10^6
1B-2	428	0.65	3.13×10^6	1.40×10^6
1B-3	464	0.50	3.38×10^6	2.08×10^6
Avg.	437	0.54	3.48×10^6	2.24×10^6
FEM	431	0.52	2.73×10^6	2.43×10^6
Diff.	2%	3%	22%	8%

Note: $Diff. = (Avg. - FEM) / FEM$

3.3 PARAMETRIC STUDY

3.3.1 Parameters investigated

To gain a thorough understanding of the mechanical behaviour and to predict the possible mechanisms of the notched connection system, a parametric study was conducted using the validated FE model. The investigated parameters were divided into two groups. The first group of parameters involved general parameters, including the concrete strength f_c , the thickness of the concrete panel h_c , and the heel length of the CLT panel l_i (see Figure 10a). On the other hand, the second group of parameters (see Figure 10b) were associated with the notched connector, including notch length l_n , notch depth d_n , and cross-sectional area of the V-shape reinforcement inside the notched connection A_s . However, the material and geometrical properties of the CLT (mechanical properties and thickness of the CLT panel) is invariable since they are fixed in the industrialized solution. Additionally, the notched angle of 59.04° is fixed to maintain the notched shape, while the V-shape rebar can be adjusted to fit inside the notched connector.



(a) First group of parameters

(b) Second group of parameters

Figure 10: Geometrical parameters studied

3.3.2 First group of parameters

Table 9 describes the details of the first group of parameters. C1, C2, and C3 simulations investigated the parameter of concrete strength, thickness of the concrete panel, and heel length of the CLT panel, respectively. In Case C3-1, the heel length of the CLT panel was increased from 187.5 mm to 375 mm.

Table 9: The details of the first group of parameters

Parameter	f_c [MPa]	h_c [mm]	l_l [mm]
Reference	35	80	187.5
C1	C1-1	25	80
	C1-2	45	187.5
C2	C2-1	35	50
	C2-2	35	100
C3	C3-1	35	80

The force-slip curves of all the cases in the first group of parameters are drawn in Figure 11. The results obtained from the numerical simulation are presented in Table 10. The value in bracket refers to the difference of peak loads in the different cases to the one in the reference case.

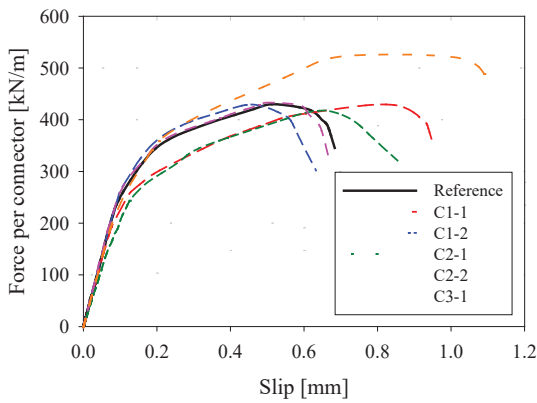


Figure 11: Force-slip curve of numerical study of C1/C2/C3

Table 10: Results obtained from numerical study of C1/C2/C3

Test	F_{max} [kN/m]	δ_{Fmax} [mm]	K_s [N/mm/m]	K_u [N/mm/m]	Failure mode
Ref.	431 (1.00)	0.52	2.73×10^6	2.43×10^6	RS
C1-1	429 (1.00)	0.78	2.58×10^6	2.03×10^6	RS
C1-2	430 (1.00)	0.45	2.73×10^6	2.63×10^6	RS
C2-1	419 (0.97)	0.66	2.17×10^6	1.96×10^6	RS
C2-2	435 (1.00)	0.48	2.87×10^6	2.62×10^6	RS
C3-1	526 (1.22)	0.72	2.51×10^6	1.95×10^6	CS

Note: RS refers to Rolling shear of the CLT while CS refers to Concrete shear of the concrete panel.

Except for Case C3-1, the failure of the notched connector was governed by the rolling shear failure of the cross-layer of the CLT panels. The maximum force ranged from 419 kN to 435 kN and was logically not influenced by the parameters related to the concrete. The maximum difference was approximately 3 percent compared to the reference case. In Case C3-1, the failure was governed by the concrete shear in the lower notched connector, even if the rolling shear stress was large in the cross-layer of the CLT panel. Figure 12 illustrates the tensile damage in the concrete panel, rolling shear stress of the CLT panel, and V-shape rebars stresses under the maximum load. The damage in the critical shear plane in the concrete was close to 1.0, while the V-shape rebars were experiencing the yielding stress (of 500 MPa) in the lower notched connector at the maximum load. It can be inferred that the simulation of Case C3-1 provides an estimation of the connection resistance on the concrete side. A 22 percent

increase in the maximum force was observed compared to reference case.

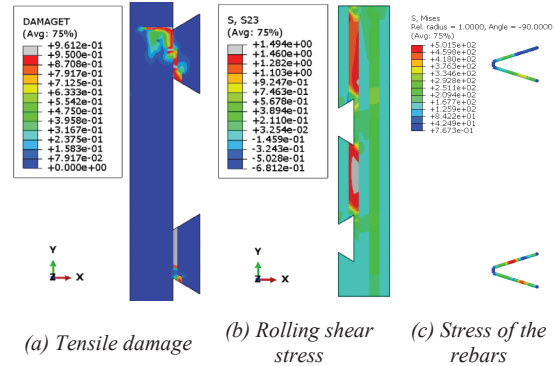


Figure 12: Tensile damage in concrete and rolling shear stress of the CLT at the maximum load in Case C3-1

In terms of the force-slip relationship, the curves exhibit similar trends in linear elastic region until a load level of approximately 270 kN. From this load level, Cases C1-1 and C2-1, which adopt lower concrete strength and smaller concrete thickness, respectively, show larger slips than other cases for the same load. The change of the parameters in these cases led to an earlier tensile damage of the concrete panel (see Figure 13). Regarding Case C3-1, a plateau of force-slip curve was noticed, starting from 0.72 mm of slip, where the first failure of the lower notched connector was obtained and ending at 0.99 mm of slip, where the other connector failed and the V-shape rebars in both notches experienced the yielding stress.

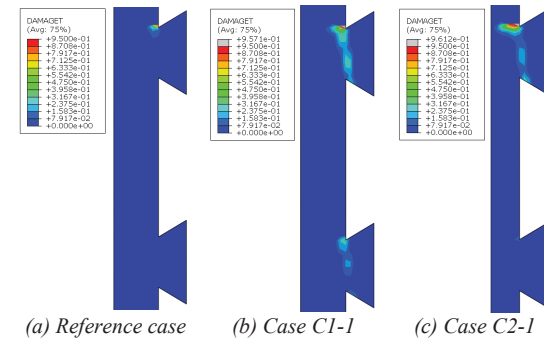


Figure 13: Tensile damage of the concrete panels at the load level of 270 kN

In addition, high stiffness was observed in both service and ultimate conditions in all cases, and slips at the maximum load of the first group ranged from 0.45 mm to 0.78 mm. In cases where the failure was related to rolling shear of the CLT panel, the ductility was limited. In case C3-1, as the maximum load was governed by the shear failure in the concrete, a higher slip of approximately 1.1 mm was achieved in Case C3-1.

Regarding other cases, it can be assumed that the concrete strength and the thickness of the concrete slab had little influence on the load bearing capacity of the notched connector since the connector behaviour was limited by the rolling shear resistance of the CLT panel. It is worth to remind that the real rolling shear resistance is lower than the experimental maximum load due to the loading

block configuration that resulted in some loading being transferred directly to the concrete panel via longitudinal compression of the CLT panel. However, lower concrete strength and smaller thickness of the concrete panel reduced the stiffness of the notched connector due to the early damage of the concrete panel.

3.3.3 Second group of parameters

The details of the parameters in the second group are described in Table 11. C4, C5, and C6 simulations investigated the influence of the notch length l_n , the notch depth d_n , and the cross-sectional area of V-shape rebar A_s , respectively. In the reference case, 5 V-shape 6-mm rebars with 90-mm spacing were used in the notched connection, corresponding to a section of 141.37 mm². For Case C6-1, no V-shape rebar was used in the notch, whereas 2 6-mm V-shape rebars were included in the notch for Case C6-2.

Table 11: The details of the second group of parameters

Parameter	l_n [mm]	d_n [mm]	A_s [mm ²]
Reference	90	50	141.37
C4	C4-1	40	141.37
	C4-2	140	141.37
C5	C5-1	90	141.37
	C5-2	90	0
C6	C6-1	90	56.55
	C6-2	90	56.55

Figure 14 presents the force-slip relationships for all the cases in the second group of parameters. The results obtained from the numerical simulation are summarized in Table 12. The same two types of failure modes were observed: rolling shear of the CLT panel and concrete shear.

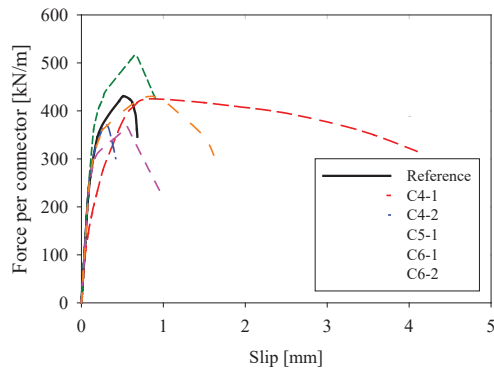


Figure 14: Force-slip curve of numerical study of C4/C5/C6

Table 12: Results obtained from numerical study of C4/C5/C6

Test	F_{max} [kN/m]	δ_{Fmax} [mm]	K_s [N/mm/m]	K_u [N/mm/m]	Failure mode
Ref.	431 (1.00)	0.52	2.73×10^6	2.43×10^6	RS
C4-1	425 (0.99)	0.85	1.51×10^6	1.11×10^6	CS
C4-2	370 (0.86)	0.30	2.88×10^6	2.80×10^6	RS
C5-1	516 (1.20)	0.65	2.78×10^6	2.54×10^6	CS
C6-1	364 (0.84)	0.53	2.63×10^6	2.60×10^6	CS
C6-2	427 (0.99)	0.75	2.68×10^6	2.36×10^6	RS+CS

Note: RS refers to Rolling shear of the CLT while CS refers to Concrete shear of concrete panel.

In cases C4, the change of notch length resulted in modifying the area of the cross layer of the CLT panel. The decrease of the notch length from 90 mm to 40 mm in Case C4-1 contributed to the higher rolling shear resistance of CLT panel and to the lower shear resistance and stiffness in the concrete. In this case, the failure was governed by the shear failure of concrete in notched connector with a maximum force of 425 kN and a corresponding slip of 0.85 mm. Figure 15 shows the damage in tension of the concrete panel and yield stress of the V-shape rebars inside the notched connection at the maximum load. From force-slip curves, Case C4-1 exhibits higher slip in the elastic region compared to other cases.

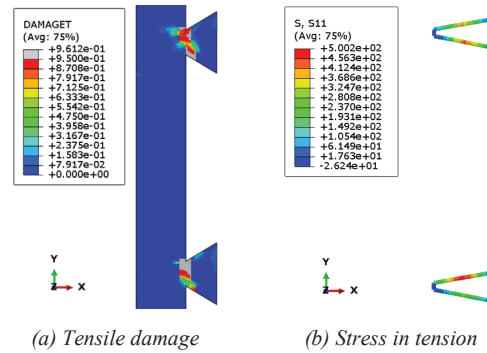


Figure 15: Concrete shear failure and stress of V-shape rebar in Case C4-1 at maximum load

Besides, Case C4-2 resulted in rolling shear failure at the maximum force of 370 kN and a corresponding slip of 0.30 mm. In this case, the increase of notched length (140 mm) led to the decrease of approximately 14 percent in rolling shear cross-section (resistance) while the corresponding slip decreased nearly two-fold. As shown in force-slip curves, the behaviour of the notched connector remained in the elastic region when the brittle failure happened in the cross-layer of CLT panel.

Decreasing the notch depth from 50 mm to 25 mm, which is smaller than the first longitudinal layer's thickness (33 mm), increases the working rolling shear section of the CLT panel in Case C5-1. This resulted in a failure that was limited by the shear failure of the concrete at a maximum force of 516 kN and a corresponding slip of 0.65 mm. It can be seen that the load bearing capacity increased by 20 percent compared to that in the reference case. The failure started from the lower notched connector, followed by the upper one as shown in Figure 16a. At the maximum load, high rolling shear stresses were found from the loading surface to the lower notched connector (blue colour) with a maximum rolling shear stress of approximately 1.49 MPa (see Figure 16b).

It should be noted that the failures in Case C5-1 of second group parameters and Case C3-1 of first group parameters, both with the same notch length, were governed by concrete shear. The maximum force in Case C3-1 was 2 percent higher compared to Case C5-1. However, the ductility of Case 3-1 is slightly better than

that of Case C5-1, possibly due to the different anchorage length of the V-shape rebars placed inside the notches.

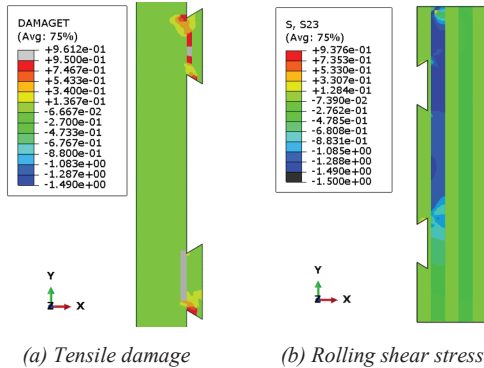


Figure 16: Tensile damage in concrete and rolling shear stress of the CLT at the maximum load in Case C5-1

The number of V-shape rebars was investigated in Case C6-1 and Case C6-2. It was found that the maximum force decreased when the amount of V-shape rebars was reduced.

The failure mode of Case C6-1 was governed by the concrete shear at the maximum force of 364 kN with a corresponding slip of 0.53 mm. The load bearing capacity decreased by 16 percent, compared to the reference case. When no shear reinforcement was placed inside the notched connector, the concrete damage started earlier, at a load level of approximately 300 kN as shown in force-slip curve (see Figure 14). At the maximum load, the upper notched connector failed first and was followed by the lower one. For the CLT panel, the highest rolling shear resistance obtained was approximately 1.43 MPa (see Figure 17).

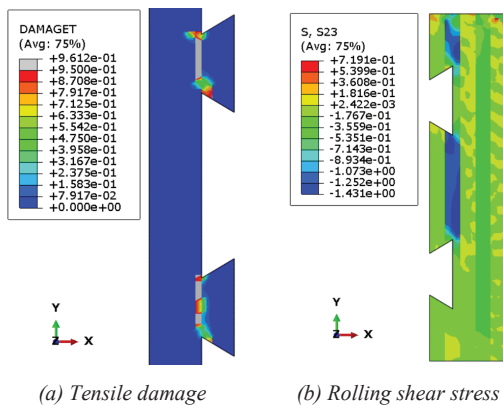


Figure 17: Tensile damage in concrete and rolling shear stress of the CLT at the maximum load in Case C6-1

In Case C6-2, the failure was initiated by concrete shear failure of the notched connector. The maximum load was obtained at 427 kN with a corresponding slip of 0.75 mm, when the upper notched connector failed. At this point, a high rolling shear stress was obtained in the cross-layer of the CLT panel.

The V-shape rebars were subjected to a tensile stress of 478 MPa at the maximum load and experienced the yield stress shortly after when the concrete of the upper notched

connector failed. The tensile damage of the concrete and the rolling shear stress of the CLT panel can be visualized in Figure 18.

In terms of stiffness, the studied parameters have minimal influence, except for the Case C4-1, in which the stiffness decreased more than half compared to the reference case. However, the notched connector in Case C4-1 can be still considered as stiff, as its stiffness is higher than the suggested value of the design slip modulus of 1.00×10^6 N/mm/m proposed in the recommendations for the design of TCC beams with notched connectors given in BNTEC [17].

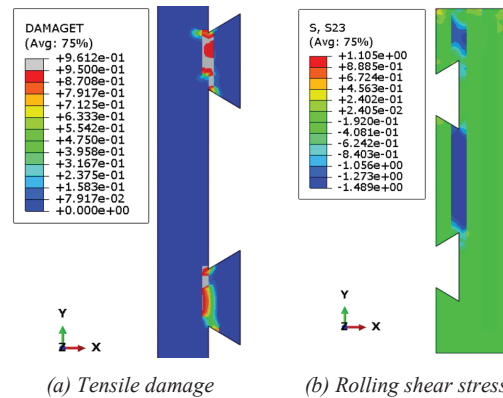


Figure 18: Tensile damage in concrete and rolling shear stress of the CLT at the maximum load in case C6-2

Regarding the ductility, no improvement was obtained by changing the values of the parameters in the second group, except for Cases C6-2 and C4-1 where ultimate slips of around 1.5 mm and 4.2 mm, respectively, were obtained.

4 CONCLUSION

This paper presents the experimental and numerical investigations on a novel notched connector for CLT-concrete composite floor systems. The pushout tests showed high shear resistance and stiffness of the connector, but low ductility, as the failure was governed by rolling shear failure of the cross-layer of the CLT panel. In addition, a full FE model of the pushout tests using ABAQUS/Explicit was established and validated against the experimental results. The simulation was capable of reproducing the failure mode of the experimental tests and giving a good agreement of force-slip curve with the results from pushout tests. The validated model was then used for a parametric study to investigate the influence of various parameters of the geometries and the materials. The following results are obtained from the parametric study:

- If not changing the notch dimensions, the strength and the thickness of the concrete panel had no significant influence on the strength, as it was governed by the rolling shear failure in cross-layer of the CLT panel. However, they had a slight effect on the stiffness of the connector, as earlier damage in the concrete notches was obtained in these cases.

- An increase of the heel length led to a larger cross-layer area of the CLT panel, and the failure was then governed by concrete shear of the notched connector. A small improvement of the post-peak behaviour was obtained. An estimation of the load provoking the concrete failure in shear was obtained. It was 22 percent larger than the mean of the experimental results.
- Decreasing the notch length from 90 mm to 40 mm was able to provoke a concrete shear failure, resulting in the improvement of the ductility of the system. Lower stiffness was found when adopting a notch length of 40 mm, but it was larger than the value suggested in BNTEC [17] for notched connections.
- A reduction of the notch depth to a value smaller than the thickness of the first longitudinal layer of the CLT panel increased the cross-section of the rolling shear of the CLT panel. This led to a higher strength and stiffness. However, low ductility was still observed.
- A higher amount of V-shape rebars increased the strength and stiffness of the notched connection.

In conclusion, based on the numerical results, it is possible to improve the ductility of the present notched connection by prioritizing the shear concrete failure of the notch, if a sufficient number of V-shape rebars are placed inside the notch. This prioritization can be obtained by increasing the spacing between the connectors, in order to increase the rolling shear resistance. The concrete failure should happen for a load 22 percent larger than the experimental resistance obtained by pushout tests. However, these conclusions need to be confirmed by additional experimental investigations.

REFERENCES

- [1] F. Schreyer, G. Felix, et al. Common but differentiated leadership: strategies and challenges for carbon neutrality by 2050 across industrialized economies. *Environmental Research Letters* 15.11 (2020): 114016.
- [2] A. Ceccotti, Timber-concrete composite structures *Timber Eng.*, 2 (1) (1995)
- [3] V. Ouch, P. Heng, Q. H. Nguyen, H. Somja, T. Soquet, a notched connection for CLT-concrete composite slabs resisting to uplift without metallic connectors: experimental investigation. *Fib Symposium 2021*, Jun 2021, Lisbon, Portugal.
- [4] ABAQUS computer software, v.6.14, Simulia, Dassault Systemes.
- [5] Avis-Technique. 3.3/17-925 v1, Panneaux bois à usages structurel – mur et plancher, Wood structural panels, 2017.
- [6] EN 408:2003-08. Timber structures – Structural timber and glued laminated timber – Determination of some physical and mechanical properties. CEN European Committee for Standardization (2003)
- [7] M. Gong, Y. H. Chui, Evaluation of Planar Shear Properties of Cross Layer in Massive Timber Panel. Report, University of New Brunswick, Fredericton, Canada, 2015.
- [8] European standard EN 1994-1-1, Eurocode 4: Design of composite steel and concrete structures - Part 1-1: General rules and rules for buildings, CEN, Brussels (2004).
- [9] A. Ceccotti, Composite concrete–timber structures. In: *Progress in structural engineering and materials*, Nethercot D et al. editors. vol. 4, No. 3; 2002. p. 264–75.
- [10] L. Cedolin, Y.R.J. Crutzen, S.D. Poli Triaxial stress–strain relationship for concrete. *ACI J*, 103 (1977), pp. 423-439
- [11] B. Alfara, F. López-Almansa, S. Oller, New methodology for calculating damage variables evolution in Plastic Damage Model for RC structures. *Eng Struct* 2017;132:70–86.
- [12] R. Hill, *The Mathematical Theory of Plasticity*, Clarendon Press, Oxford, 1950.
- [13] A. Dias, J.W. Van de Kuilen, S. Lopes, et al., A non-linear 3D FEM model to simulate timber–concrete joints, *Adv. Eng. Softw.* 38 (8–9) (2007) 522–530.
- [14] T. Kartheek, T. V. Das, 3D modelling and analysis of encased steel-concrete composite column using ABAQUS. *Materials Today: Proceedings*, 27, 1545-1554. using ABAQUS. *Materials Today: Proceedings*, 27 (2020), 1545-1554.
- [15] J.R. Aira, F. Arriaga, G. Íñiguez-González, J. Crespo Static and kinetic friction coefficients of Scots pine (*Pinus sylvestris*), parallel and perpendicular to grain direction *Mater Constr*, 64 (315) (2014), p. e030
- [16] J.W.G. Van de Kuilen, M. Dejong, 3D-numerical modelling of DVW-reinforced timber joints. In: *Proceedings of WCTE 2004 – World Conference on Timber Engineering*, Espoo Finland (CD Rom); 2004.
- [17] Bureau de normalisation (BNETC), BNTEC P21A N376 Projet final TS Mixte Bois béton, BNTEC, 2020.